SIX DAYS ■ THREE CONFERENCES ■ ONE EXHIBITION

EUROPEAN MICROWAVE WEEK 2019
PARIS EXPO PORTE DE VERSAILLES, PARIS, FRANCE
1 place de la Porte de Versailles
29TH SEPTEMBER - 4TH OCTOBER 2019

EUROPEAN MICROWAVE WEEK
PORTE DE VERSAILLES
PARIS, FRANCE
29TH SEPT - 4TH OCT 2019
www.eumweek.com

EuMW 2019

EUROPEAN MICROWAVE WEEK 2019

CONFERENCE PROGRAMME

EUROPE'S PREMIER MICROWAVE, RF, WIRELESS AND RADAR EVENT

Register online at:
www.eumweek.com

EuMA
European Microwave Association

Official Publication: Journal

Organised by: horizon house

Supported by: IET

Co-sponsored by: MTT-S

Co-sponsored by: IEEE

EuMIC 2019
The 14th European Microwave Integrated Circuits Conference
Co-sponsored by:

49TH EUROPEAN MICROWAVE CONFERENCE 2019
The 49th European Microwave Conference
Co-sponsored by: EurAAP

EuRAD 2019
The 16th European Radar Conference
Co-sponsored by: EurAAP AESS

49th EUROPEAN MICROWAVE CONFERENCE 2019

49th EUROPEAN MICROWAVE CONFERENCE 2019

	E04	E05
	EuMC23 **Millimeter-wave Transition Structures and Packaging Techniques** Chair: Mehmet Kaynak[1] Co-Chair: Claire Dalmay[2] [1]IHP, 15236, Frankfurt (Order), Germany, [2]XLIM Research Institute, University of Limoges, Limoges, France	**EuMC24** **Planar Filters II** Chair: Roberto Gómez-García[1] Co-Chair: Dimitra Psychogiou[2] [1]University of Alcala, [2]University of Colorado Boulder
13:50 - 14:10	***EuMC23-1*** ***D-band Silica-Based Package Substrate with EBG Structure for Flip-Chip Modules*** Masaharu Ito[1], Tsunehisa Marumoto[1] [1]NEC Corporation	***EuMC24-1*** ***Compact Square/Triangle Mixed-Shape Quarter-Mode Substrate Integrated Waveguide Bandpass Filter with Wide Stopband*** Phirun Kim[1], Wang Qi[1], Phanam Pech[1], Junhyung Jeong[1], Yongchae Jeong[1] [1]Chonbuk National University
14:10 - 14:30	***EuMC23-2*** ***F-band Low-loss Tapered Slot Transition for Millimeter-wave System Packaging*** Ahmed Hassona[1], Zhongxia Simon He[1], Vessen Vassilev[1], Herbert Zirath[1] [1]Chalmers University of Technology	***EuMC24-2*** ***Multilayered Wideband Balun Bandpass Filters Designed with Input-Reflectionless Response*** Li Yang[1], Roberto Gómez-García[1], José-María Muñoz-Ferreras[1], Wenjie Feng[2] [1]University of Alcala, [2]Nanjing University of Science and Technology
14:30 - 14:50	***EuMC23-3*** ***A Compact 28 GHz RF Front-end Module using IPDs and Wafer-level Metal Fan-out Packaging*** Jongmin Yook[1] [1]KETI (Korea Electronics Technology Institute)	***EuMC24-3*** ***Topology and Rigorous Design Method for Reflectionless Bandstop Filter*** Jongheun Lee[1], Boyoung Lee[1], Seunggoo Nam[1], Juseop Lee[1] [1]Korea University
14:50 - 15:10	***EuMC23-4*** ***Broadband Stacked-Patch Transition from Microstrip Line to Circular Dielectric Waveguide for Dual-Polarized Applications at W-Band Frequencies*** Andre Meyer[1], Martin Schneider[1], Simon Karau[1] [1]Universität Bremen	***EuMC24-4*** ***Magnet-less Non-Reciprocal Bandpass Filters With Tunable Center Frequency*** Dakotah Simpson[1], Dimitra Psychogiou[1] [1]University of Colorado at Boulder
15:10 - 15:30	***EuMC23-5*** ***A Novel Miniaturized High Performance BGA RF Transition for Ka Band Applications*** Firat Altuntas[1] [1]Aselsan Inc.	***EuMC24-5*** ***Design of Wideband Bandpass Filters Using Parallel-Coupled Asymmetric Three Line Structures with Adjustment Elements*** Elif Güntürkün Şahin[1], Ali Kursad Gorur[2], Ceyhun Karpuz[3], Adnan Gorur[1] [1]Nigde Omer Halisdemir University, [2]Nevsehir Haci Bektas Veli University, [3]Pamukkale University

Compact Square/Triangle Mixed-Shape Quarter-Mode Substrate Integrated Waveguide Bandpass Filter with Wide Stopband

Phirun Kim[#1], Qi Wang[#], Phanam Pech[#], Junhyung Jeong[#], and Yongchae Jeong[#2]

[#]Division of Electronics and Information Engineering, Chonbuk National University, Jeonju-si, Republic of Korea

[1]fmphirun@jbnu.ac.kr, [2]ycjeong@jbnu.ac.kr

***Abstract*—In this paper, a new square/triangle mixed-shape quarter-mode substrate integrated waveguide (SIW) bandpass filter (BPF) is presented. Two transmission poles in the passband and two transmission zeros (TZs) in the stopband can be obtained by using a mixed quarter-mode cavity sharp. For an experimental validation, two-stage with square/triangle mixed-shape quarter-mode SIW BPF is designed at the center frequency (f_0) of 8 GHz. From measurements, the insertion loss (S_{21}) and return loss (S_{11}) of 1.1 dB and 15.1 dB are obtained at f_0, respectively. The passband insertion loss is better than 1.3 dB in the bandwidth of 0.87 GHz (7.55 ~ 8.42 GHz). The return losses better than 15.1 dB for the same bandwidth is measured. The two TZs in stopband make the attenuation characteristics better than 39.6 dB and 33 dB at 11.44 GHz and 15.67 GHz, respectively. And the proposed SIW BPF is compact due to mixed-shape quarter-mode shape.**

Keywords*—bandpass filter, quarter-mode resonator, substrate integrated waveguide.

I. INTRODUCTION

Bandpass filters (BPFs) with compact-size, low-cost, and high performances are researched and developed dramatically in recent years. Substrate integrated waveguide (SIW) BPF is one of the planar circuits that can provide high Q-factor, low-loss, working on low/high frequency, high power-handling capability, and easy integration with other planar circuits [1].

The SIW circuit has been developed for various purposes using full-mode, half-mode, and quarter-mode cavities to design BPF and antennas [2]-[12]. In [2], the SIW BPF has been designed at millimeter wave using full-mode cavities with magnetic and electric couplings. The SIW impedance transformer is presented in [3] using a full-mode cavity. The impedance transforming ratio can be controlled by changing the input/output couplings. In [4], the oversized SIW cavities are used to design BPF with multiple transmission zeros (TZs) without cross-coupling structure. Moreover, the stopband attenuation is also improved. Similarly, the dual-mode cavities and air-filled SIW BPF with multiple TZs are presented in [5]. The resonance frequency of the cavity can be controlled by removing dielectric substrate partially of the SIW cavity. In [6], dual-mode circular SIW BPF designed with different size cavities and two extra via-hole inside the cavities produces transmission poles (TPs) and controllable TZs without cross-coupled resonators. Similarly, the circular cavity with cross-coupled resonators is designed to produce TZs near to the passband with high selectively performance [7]. Since the full-mode cavity has a large circuit size, the quarter-mode resonator is analyzed and can reduce a circuit size up to 75% compared to a full-mode cavity [8]. With this benefit, the quarter-mode SIW cavities are used to design antennas [9] and sub-array antennas [10]. On the other hand, the quarter-mode cavity SIW is also used to design BPF with a very compact circuit size. In [11], one-quarter of the square shape SIW cavity is analyzed and used to design SIW BPF with different coupling mechanisms of the cavity. Moreover, single-band and dual-band SIW BPFs with one-third-mode of triangle cavity is proposed [12]. The dual-band BPF can be obtained by making two extra inductive windows at the edge of the resonators.

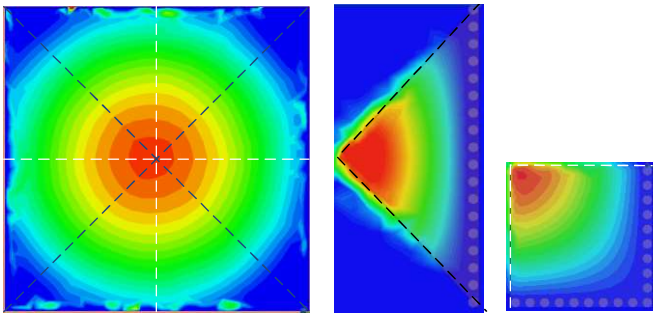

(a) (b) (c)

Fig. 1. SIW resonators: (a) full-mode cavity, (b) triangle quarter-mode cavity, and (c) square quarter-mode cavity.

In this paper, a square/triangle mixed-shape quarter-mode SIW BPF is proposed. The quarter-mode square cavity is coupled to the quarter-mode triangle shape cavity by using a magnetic coupling that controlled with a sharing iris window. The obtained TZs can improve stopband attenuation characteristic by using square/triangle mixed-shape quarter-mode cavities. Moreover, the circuit size of the proposed filter is compact.

Fig. 2. Coupling structure of coupled resonators bandpass filter.

II. Quarter-Mode SIW Resonators

Fig. 1 shows the SIW resonators with full-mode, quarter-mode with triangle, and quarter-mode with square structure, respectively. The quarter-modes of triangle and square structures have been analyzed and used in filter and antenna designs [8], [10]-[13]. The quarter-mode triangle cavity has one electric sidewall and two magnetic sidewalls. However, the quarter-mode square cavity has two electric sidewalls and two magnetic sidewalls. Both cavities have the same resonance frequency with a size only one-quarter of the full-mode resonator structure as shown in Fig. 1. The general SIW BPFs are designed using the magnetic coupling with a sharing via-hole window. For the proposed filter, the quarter-modes with square /triangle structure cavities are designed together. By mixing both resonators, the TZs in the stopband can be obtained and provided a wide stopband characteristic.

For the proposed filter, the general coupling structure of the coupled resonators is shown Fig. 2. r_1 to r_n are the resonators. S and L stand for source and load terminations ($Z_S = Z_L = Z_0$). Q_{eS} and Q_{eL} are the external quality factor at the source and load, respectively. Moreover, $K_{i,i+1}$ is a coupling coefficient between i-th and i+1-th resonators. The $Q_{eS,eL}$ and $K_{i,i+1}$ can be calculated from (1) [1].

$$Q_{eS} = Q_{eL} = \frac{g_{0,n}g_{1,n+1}}{\text{FBW}} \tag{1a}$$

$$K_{i,i+1} = \frac{\text{FBW}}{\sqrt{g_i g_{i+1}}} \tag{1b}$$

where g_0, g_1, ⋯, and g_{n+1} are the low-pass prototype element values. FBW is the fractional bandwidth of the passband.

The electromagnetic (EM) simulation is used to extract the Q_{eS}, Q_{eL}, and $K_{i,i+1}$ by the following equations (2) and (3)-(4), respectively.

$$Q_{eS,eL} = \frac{f_0}{\Delta f_{\pm 3\text{dB}}}, \tag{2}$$

where $\Delta f_{\pm 3\ \text{dB}}$ is the 3-dB bandwidth of the center frequency (f_0). Moreover, $K_{i,i+1}$ can be calculated from (3) for the tuned coupled resonator synchronously.

$$K_{i,i+1} = \frac{f_{p2}^2 - f_{p1}^2}{f_{p2}^2 + f_{p1}^2}, \tag{3}$$

where i is a value in the range of 2 to n-1. Similarly, the coupling coefficient between two resonators (K_{12} and $K_{n,n+1}$) can be calculated from (4) for the asynchronous case.

$$K_{1,2} = K_{n-1,n} = \pm\frac{1}{2}\left(\frac{f_{R_1}}{f_{R_2}} + \frac{f_{R_2}}{f_{R_1}}\right)\sqrt{\left(\frac{f_{p_2}^2 - f_{p_1}^2}{f_{p_2}^2 + f_{p_1}^2}\right)^2 - \left(\frac{f_{R_2}^2 - f_{R_1}^2}{f_{R_2}^2 + f_{R_1}^2}\right)^2} \tag{4}$$

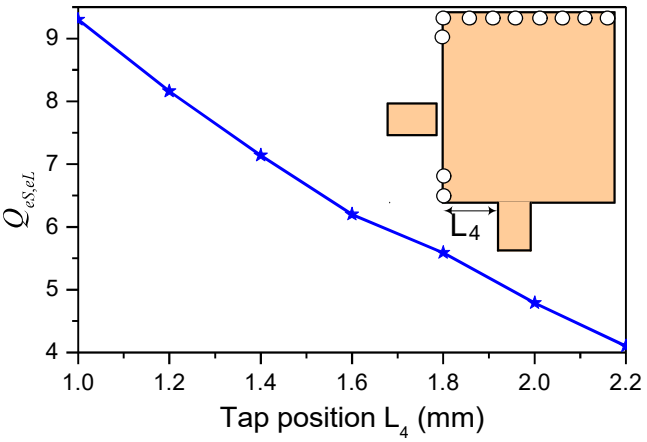

Fig. 3. Extracted quality factor according to tap position of square cavity.

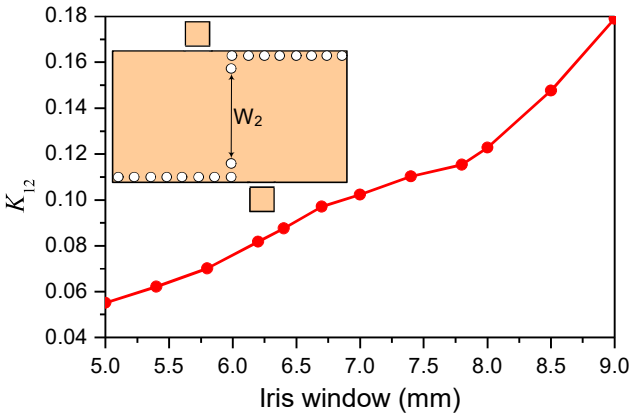

Fig. 4. Extracted coupling coefficient K_{12} according to iris window width of the square/square cavities SIW BPF.

where f_{Rj} (j = 1, 2) is a self-resonance frequency and f_{pj} is the two split resonant frequencies.

To verify the proposed filter, two SIW BPFs have been designed to operate at f_0 of 8 GHz with passband ripple of 0.043 dB, two-stage resonators, and FBW of 9%. One filter is designed with quarter-mode square/square cavities and other filter is designed with mix square/triangle cavities. The filter is designed on RT/Duriod 5880 substrate with dielectric constant (ε_r) of 2.2 and thickness (h) of 0.52 mm. From [1], $g_0 = 1$, $g_1 = 0.6648$, $g_2 = 0.5445$, and $g_3 = 1.221$ are extracted for 0.043 dB of the passband ripple. According to (1), the $Q_{eS} = Q_{eL} = 7.387$ and $K_{12} = 0.1496$ are calculated.

Using EM simulation, the $Q_{eS,eL}$ according to the tap position (L_4) of the square cavity can be extracted and calculated using (2), as shown in Fig. 3. The $Q_{eS,eL}$ is controlled by tapping from the short-circuit of via-hold [1]. It is note that $Q_{eS,eL}$ is decreased as the tap position from the via-hold increases. Similarly, the coupling coefficient (K_{12}) of the square/square cavities is extracted from the EM simulation using (3)-(4). Fig. 4 shows the K_{12} according to the width of a sharing iris window (W_2). As can be seem, the K_{12} is increased as the width of iris window increases.

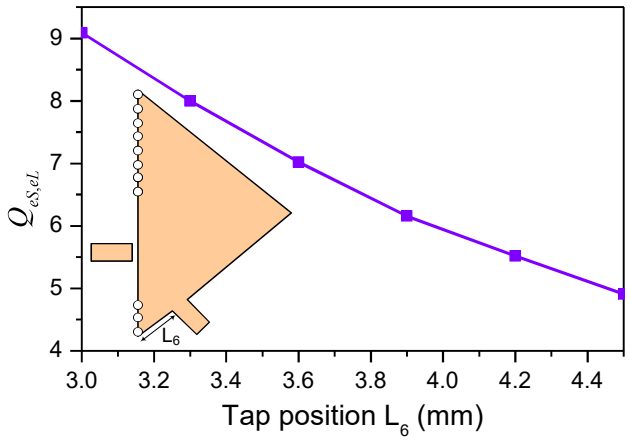

Fig. 5. Extracted quality factor according to tap position of triangle cavity.

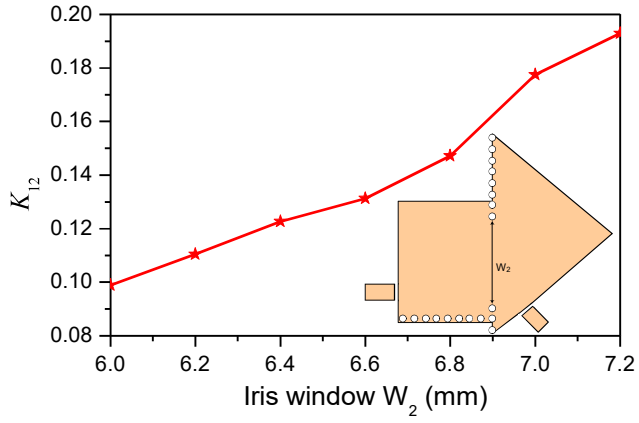

Fig. 6. Extracted coupling coefficient K_{12} according to iris window width of the square/triangle cavities SIW BPF.

For the mixed of square/triangle cavities, the designed processes are the same. The $Q_{eS,eL}$ of the square/triangle cavities can be extracted from the EM simulation by controlling a tap position as shown in Fig. 5. As can be seem, the $Q_{eS,eL}$ is decreased as the tap position from the via-hold increases. Moreover, the quarter-mode square cavity is coupled to the bottom of quarter-mode triangle cavity and controlled by a sharing iris window width (W_2) as can seem in Fig. 6. As can be seem, the K_{12} is increased as the W_2 increases.

Fig. 7 shows layout of two-stage quarter-mode with square/square and square/triangle cavities SIW BPFs. Two SIW BPFs are designed with the same specifications as mentioned early. According to calculation $Q_{eS} = Q_{eL} = 7.387$ and $K_{12} = 0.1496$ are required for the specifications. From Figs. 3, 4, 5, and 6, the tap position and iris window width are extracted. The final physical lengths are shown in Figs. 7(a) and 7(b) for square/square and square/triangle cavities SIW BPFs, respectively. Similarly, Fig. 8 shows the *S*-parameters comparison of both filters. From the simulation, the quarter-mode SIW BPF with square/square cavities produces a

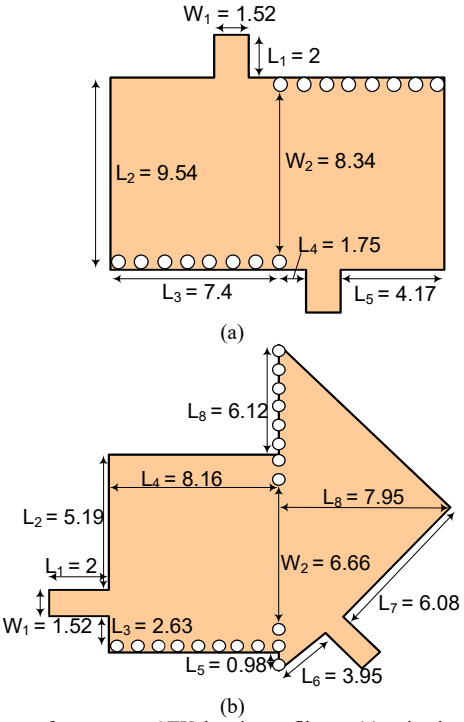

Fig. 7. Layout of two-stage SIW bandpass filters: (a) mixed square/square cavities and (b) square/triangle cavities. (unit: mm)

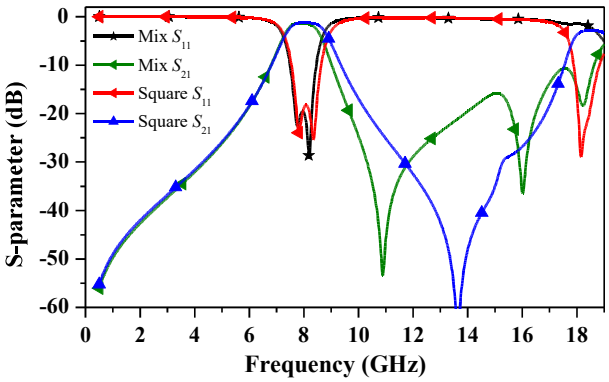

Fig. 8. EM simulation of two-stage quarter-mode SIW BPF with square/square and square/triangle cavities.

spurious frequency at 18 GHz ($2.25f_0$) with a TZ at 13.6 GHz. Moreover, two TPs in the passband are obtained with FBW of 8.5% (8.39-7.71 GHz). However, the quarter-mode SIW BPF with square/triangle cavities also produce two TPs in the passband. The first and second TZs are produced by the triangle and square cavities, respectively. The second TZ is located at the second passband ($2f_0$) which is useful in RF system performance. Moreover, the spurious frequency of proposed filter is located higher than the square cavity filter. Thus, the proposed quarter-mode SIW BPF with square/triangle cavities provides extra TZs, higher selectivity and higher spurious frequency with a compact circuit size.

III. Simulation and Measurement

To validate the proposed filter, two-stage quarter-mode SIW BPF with square/triangle cavities resonator is designed and fabricated.

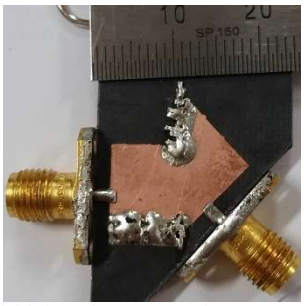

Fig. 9. Photograph of fabricated quarter-mode SIW BPF with square/triangle cavities.

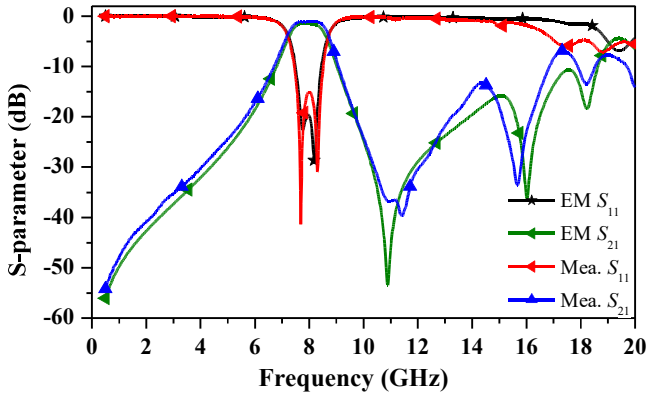

Fig. 10. *S*-parameters of proposed quarter-mode SIW BPF with square/triangle cavities.

The filter is designed with the same specifications and substrate as mentioned in the early section. The layout of proposed filter is shown in Fig. 7(b).

Fig. 9 shows the photograph of the fabricated two-stage quarter-mode SIW BPF. The overall size of the proposed circuit is 16.76 mm × 18.11 mm. The simulated and measured *S*-parameters of the proposed filter are shown in Fig. 10. The measured input return loss is better than 15.1 dB at the f_0. Moreover, the return loss better than 15.1 dB is measured within the operating band of 7.55-8.42 GHz (FBW = 10.89%). The measured insertion loss (S_{21}) at the f_0 is 1.1 dB, showing a good agreement with the simulation result. Within the same passband, the measured insertion loss is better than 1.3 dB. The fabricated filter provides a wide stopband attenuation with two TZs. The TZs at 11.44 GHz (1.43f_0) and 15.67 GHz (1.95f_0) are measured and attenuated better than 39.6 dB and 33 dB, respectively. The attenuation at the lower stopband is measured better than 15 dB from dc to 6.25 GHz. Similarly, the attenuation at the higher stopband is measured better than 13 dB from 9.26 GHz to 16.63 GHz. Moreover, the spurious frequency of proposed filter is located higher than the 18 GHz (2.25f_0).

IV. Conclusion

In this paper, a quarter-mode SIW BPF with square/triangle cavities resonators is presented. Both the simulation and measurement results are provided to validate the proposed circuits. The circuit size of proposed filter is compact about 75% smaller than full-mode resonators. The proposed filter of square/triangle mixed-shape quarter-mode cavities can produce two TZs in the stopband. Moreover, the first spurious frequency is occurred far away from the fundamental. The proposed filter is simple structure to design in microstrip.

References

[1] J.-S. Hong, *Filters for RF/microwave applications*, 2nd edition, John Wiley & Sons, Inc., 2011.

[2] K. Wang, S.-W. Wong, G.-H. Sun, Z. Chen, L. Zhu, and Q.-X. Chu, "Synthesis method for substrate-integreted waveguide bandpass filter with even-order chebyshev response," *IEEE Trans. Compon. Packanging Manufact. Technol.*, vol. 6, no. 1, pp. 126-135, Jan. 2016.

[3] J. Jeong, P. Kim, P. Pech, Y. Jeong, and S. Lee, "Substrate-integrated waveguide impedance matching network with bandpass filtering," *2019 IEEE Radio Wireless Sympos.*, Orlando, Florida, Jan. 2019.

[4] X.-P. Chen, K. Wu, and D. Drolet, "Substrate integrated waveguide filter with improved stopband performance for satellite ground terminal," *IEEE Trans. Microwave Theory Techn.*, vol. 57, no. 3, pp. 674-683, Mar. 2009.

[5] C. Tomassoni, L. Silvestri, A. Ghiotto, M. Bozzi, and L. Perregrini, "Substate-integrated waveguide filters basded on dual-mode air-filled resonant cavities," *IEEE Trans. Microwave Theory Techn.*, vol. 66, no. 2, pp. 726-736, Feb. 2018.

[6] F. Cheng, X. L. Lin, M. Lancaster, K. Song, and Y. Fan, "A dual-mode substrate integrated waveguide filter with controllable transmission zeros," *IEEE Microw. Wireless Components Lett.*, vol. 25, no. 9, pp. 576-578, Sep. 2015.

[7] N. Delmonte, M. Bozzi, L. Perregrini, and C. Tomassoni, "Cavity resonator filters in shielded quarter-mode substrate integrated waveguide technology," *IEEE MTT-S International Microw. Workshop Series Advanced Materials Processes for RF and THz Application*, Jul. 2018.

[8] S. Zhang, H.-T. Wang, J.-Y. Rao, X.-D. Fu, and F.-L. Liu, "Cross-coupled bandpass filter based on circular subtrate integrated waveguide resonator," *IEICE Electronics Express*, vol. 13, no. 22, pp. 1-7, Nov. 2016.

[9] C. Jin, Z. Shen, R. Li, and A. Alphones, "Compact circularly polarized antenna based on quarter-mode substrate integrated waveguide sub-array," *IEEE Trans. Antennas Propag.*, vol. 62, no. 2, pp. 963-967, Feb. 2014.

[10] C. Jin, R. Li, A. Alphones, and X. Bao, "Quarter-mode substrate integrated waveguide and its application to antennas design," *IEEE Trans. Antennas Propag.*, vol. 61, no. 6, pp. 2921-2928, Jun. 2013.

[11] S. Moscato, C. Tomassoni, M. Bozzi, and L. Perregrini, "Quarter-mode cavity filters in substrate integrated waveguide technology," *IEEE Trans. Microwave Theory Techn.*, vol. 64, no. 8, pp. 2538-2547, Aug. 2016.

[12] S. Zhang, J.-Y. Rao, J.-J. Cheng, X.-D. Fu, F.-L. Liu, and J.-S. Hong, "Novel compact single-band and dual-band bandpass filter based on one-third-mode substrate integrated waveguide," *IEICE Electronics Express*, vol. 14, no. 19, pp. 1-6, Sep. 2017.

[13] C. Jin and Z. Shen, "Compact triple-mode filter based on quarter-mode substrate integrated waveguide," *IEEE Trans. Microwave Theory Techn.*, vol. 62, no. 1, pp. 37-45, Jan. 2014.